New Processes in the Environmental Chemistry of Nitrite: Nitration of Phenol upon Nitrite Photoinduced Oxidation

ARTICLE *in* ENVIRONMENTAL SCIENCE AND TECHNOLOGY · MARCH 2002

Impact Factor: 5.33 · DOI: 10.1021/es010101c · Source: PubMed

4 AUTHORS, INCLUDING:

Davide Vione
Università degli Studi di Torino
265 PUBLICATIONS **3,749** CITATIONS
SEE PROFILE

Valter Maurino
Università degli Studi di Torino
203 PUBLICATIONS **4,005** CITATIONS
SEE PROFILE

Claudio Minero
Università degli Studi di Torino
329 PUBLICATIONS **8,126** CITATIONS
SEE PROFILE

Environ. Sci. Technol. **2002**, *36,* 669−676

New Processes in the Environmental Chemistry of Nitrite: Nitration of Phenol upon Nitrite Photoinduced Oxidation

DAVIDE VIONE, VALTER MAURINO, CLAUDIO MINERO, AND EZIO PELIZZETTI*

Dipartimento di Chimica Analitica, Università di Torino, Via P. Giuria 5, 10125 Torino, Italy

The role of nitrite as an environmental factor has been widely recognized. Nitrite is a relevant source of •OH in the atmosphere, both in the gas phase via photolysis of gaseous HNO_2 and in atmospheric hydrometeors by photolysis of NO_2^-. In aqueous systems, •OH production through nitrite photolysis can be negligible due to the competition for light absorption by dissolved Fe(III), colloidal iron oxides, and nitrate. These photoexcited oxidants interact with NO_2^- and HNO_2 to form $•NO_2$, either directly or via formation of •OH. As a consequence, nitrite and nitrous acid may act as $•NO_2$ rather than •OH sources. The radical $•NO_2$ is involved in the nitration of many aromatic compounds, of which phenol is a model in this work. Kinetic measurements using 2-propanol as •OH scavenger show that the direct production of •OH by aqueous Fe(III) species decreases as pH increases. At slightly acidic and neutral pH values, oxidation of nitrite occurs by direct electron transfer to photoexcited $Fe(III)_{aq}$ species or colloidal iron oxides, in addition to the •OH-mediated oxidation of NO_2^-. The reported findings suggest a completely new role of nitrite in aquatic environments.

Introduction

Nitrite is a relevant environmental factor both in natural waters (*1*−*4*) and in the atmosphere (*5*). Up to now, the attention was mainly focused on nitrite UV photolysis, leading to hydroxyl radical and nitrogen monoxide (*6*):

$$NO_2^- + h\nu \rightarrow •NO + •O^- \quad [\Phi_{310\ nm} \approx 0.06] \qquad (1a)$$

$$•O^- + H^+ \leftrightarrows •OH \quad [pK_{a,1b} = 11.9] \qquad (1b)$$

As far as nitrite is the only photoactive species, it can play a dual role. Besides being a source of •OH, nitrite can act as a sink for the same radicals, reacting with them at a diffusion-controlled rate giving $•NO_2$ as product (*6*):

$$•OH + NO_2^- \rightarrow •NO_2 + OH^- \quad [k_2 = 1.0 \times 10^{10}\ M^{-1}\ s^{-1}] \qquad (2)$$

Nitrogen dioxide promotes the nitration of a variety of organic compounds. Phenol (*7*−*11*) and various azaarenes (*3*) can be nitrated directly by $•NO_2$, whereas the nitration of benzene (*12*) and various PAHs (*13*) is assisted by •OH. Other aromatic molecules of environmental concern that can be nitrated are resorcinol, catechol, hydroquinone, biphenyl, and some of its derivatives (*2*). However, reaction 2 becomes significant only if $[NO_2^-]$ is considerably higher than the usual nitrite concentration in the environment. Nitration of phenol (*14*) and various azaarenes (*3*) upon nitrite photolysis is actually possible but only at high $[NO_2^-]$ (up to 0.1 M).

Environmental factors have often been studied separately, although most environmental processes are the result of very complex interactions among several species. As a consequence, the study of the interactions between the various environmental factors is of foremost importance to the understanding of real environmental processes.

We recently demonstrated that phenol photonitration in the presence of nitrite is enhanced by TiO_2 in aqueous suspension (*15*). Titanium dioxide is both a promising photocatalyst for water detoxification (*16*) and an environmental factor (*1*). The reactive species in TiO_2 photocatalysis are surface adsorbed hydroxyl radicals, free or trapped valence band holes (*17*), and conduction band electrons, which promote the redox processes of many dissolved molecules.

The reaction causing the enhancement of phenol nitration in the presence of TiO_2 is very similar to reaction 2. Photogenerated species on TiO_2 particles ($•OH_{ads}$) perform like homogeneous •OH (*15*, *17*). As a consequence, the rate of light-induced •OH generation is no longer limited by NO_2^- photolysis and thus by $[NO_2^-]$ (see reaction 1). The concentration of nitrite only influences the formation rate of $•NO_2$. Thus, the generation rate of $•NO_2$ can be relevant at nitrite concentrations lower than in the case of nitrite photolysis. This has a potential environmental significance. In this framework, an interesting point is whether titanium dioxide is a unique case or also other substances present in the environment can induce the same processes.

In this paper, we report on the effects of dissolved Fe(III), α-Fe_2O_3, β-FeOOH, NO_3^-, and humic acid on phenol nitration in irradiated systems containing NO_2^-. Actually, the formation of toxic nitroderivatives, in particular in the atmosphere, is of concern for the consequences on human health (*18*) and the environment (*19*). For instance, 3-nitrobenzanthrone and 1,8-dinitropyrene are the most powerful direct mutagens so far detected in atmospheric particulate (*20*).

Phenol was chosen as a model aromatic molecule. Phenol nitration takes place via reaction with $•NO_2$ or N_2O_4 ($[N_2O_4] \propto [•NO_2]^2$ (*2*, *7*−*10*)) or the oxidation of nitrosoderivatives (*14*). The first pathway, which has more general environmental significance, involves the generation of nitrogen dioxide by nitrite oxidation. Accordingly, the significance of the second mechanism was assessed by evaluation of the oxidation rate of 4-nitrosophenol to 4-nitrophenol under the same experimental conditions used for phenol nitration.

Experimental Section

Reagents and Materials. Phenol (P), 2-nitrophenol (2-NP), 4-nitrophenol (4-NP), 4-nitrosophenol (4-NOP) (purity grade >98%), and humic acid sodium salt were purchased from Aldrich, $NaNO_2$ (>97%) and $FeSO_4 \times 7H_2O$ (99.5%) from Carlo Erba, $Fe(ClO_4)_3 \times 9H_2O$ (>97%) from Fluka, $NaNO_3$ (>99%), $HClO_4$ (70%), and HNO_3 (65%) from Merck. All reagents were used as received without further purification. Acetonitrile and 2-propanol were LiChrosolv gradient grade, purchased from Merck. α-Fe_2O_3 and β-FeOOH have been synthesized following the procedure given by Leland and Bard (*21*).

* Corresponding author phone: +39-011-6707630; fax: +39-011-6707615; e-mail: pelizzet@ch.unito.it.

10.1021/es010101c CCC: $22.00
Published on Web 01/15/2002

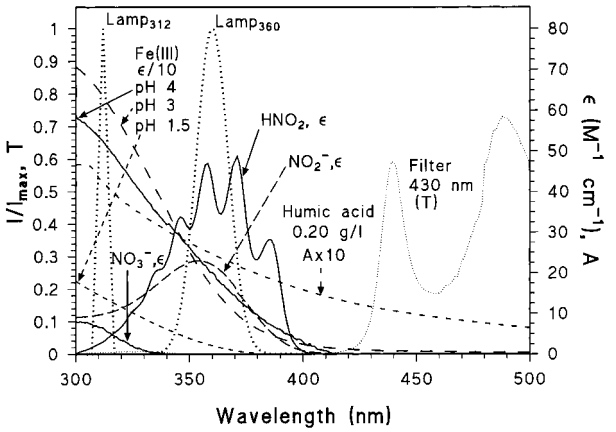

FIGURE 1. Irradiance spectra of the lamps Philips TL 01 (max. at 312 nm) and Philips TL K 05 (max. at 360 nm); transmission spectrum of the 430-nm filter; molar absorption coefficient ϵ (M^{-1} cm^{-1}) of $Fe(ClO_4)_3$ (pH 1.5, 3.0, and 4.0), HNO_2 (pH 1.5), $NaNO_2$ (pH 6.5), $NaNO_3$ (pH 6); absorbance of humic acid 0.20 g/L (pH 6).

Irradiation Experiments. Irradiation was carried out in cylindrical Pyrex glass cells (4.0 cm diameter, 2.3 cm height), containing 5 mL of aqueous solution (or suspension).

The following radiation sources were used: (i) a set of 3 × 40 W Philips TL K05 lamps with emission maximum at 360 nm. Total photon flux in the cells was 3.8×10^{-7} Ein s^{-1}, actinometrically determined using the ferrioxalate method (*22*); (ii) a 100 W Philips TL 01 lamp (emission maximum 312 nm), producing a photon flux of 1.3×10^{-7} Ein s^{-1} in the cells; (iii) a Solarbox (CO.FO.ME.GRA., Milan, Italy) with a 1500 W Philips Xenon lamp, equipped with a 430 nm filter. The lamp produces a photon flux of 4.4×10^{-6} Ein s^{-1} in the cells in the wavelength interval 430−510 nm.

The emission spectra of the lamps, together with the absorption spectra of the species of interest, are reproduced in Figure 1 and will be discussed in the following section.

After irradiation, the solutions were directly analyzed, while the suspensions were first filtered through 0.45 μm filter membranes (cellulose acetate, Millipore).

Analytical Determinations. The HPLC determinations were carried out on a Hitachi HPLC chromatograph, using a RP-C18 LichroCART column (Merck, length 125 mm, diameter 4 mm) packed with LiChrospher 100 RP-18 (5 μm diameter).

Phenol, nitrophenols, and 4-nitrosophenol were isocratically eluted with a 30/70 mixture of acetonitrile/NaH_2PO_4 (2×10^{-2} M, pH 5.5) and detected at 210 nm. Under these conditions the retention times were (min) as follows: P (3.75), 2-NP (9.30), 4-NP (5.10), and 4-NOP (2.05). The retention time corresponding to the void volume was 0.89 min.

Absorbed Light Calculations. When several absorbing species are present in the same solution, they compete for light absorption. From the Beer's law $dI_{abs}(x) = -\sum_i \mu^i \times I(x) \times dx$, where $\mu^i = 2.303 \times \epsilon^i \times c^i$, and the radiation balance $I_0 = I(x) + \sum_i I_{abs}{}^i(x)$, it follows a set of i first-order ordinary differential equations, which solved give the absorptance $\alpha^i(b)$, that is the fraction of light absorbed by each single species i in the mixture (*23*), as a function of the optical path b:

$$\alpha^i(b) = \frac{I_{abs}{}^i(b)}{I_0} = \frac{\mu^i}{\sum_j \mu^j}(1 - e^{(-b\sum_j \mu^j)}) \qquad (3a)$$

Equation 3a shows the dependence of absorptance from previously determined or known ϵ^i, and it is equivalent to the well-known eq 3b (*24*)

$$\alpha^i(b) = \frac{A^i}{A_{tot}}(1 - T) \qquad (3b)$$

where A^i, A_{tot}, and T are the actual absorbance of the species i ($A^i = \epsilon^i c^i b$), and the (total) absorbance and transmittance of the mixture, respectively. Equations 3a,b strictly hold for monochromatic radiation. However, if the light beam contains radiation in a narrow wavelength interval (which is the case of light from the 312 and 360 nm emission sources used in this work), and ϵ^i may be considered almost constant in the narrow wavelength interval considered, eqs 3a,b are a good approximation for photochemical calculations. In our case the optical path was $b = 0.4$ cm.

Determination of the Initial Rates and the Relative Uncertainty. The disappearance of phenol and the formation of nitrophenols were followed for different irradiation times. The time evolution of phenol concentration [Ph] follows with good approximation a pseudo-first-order kinetics

$$[Ph] = [Ph]_0 \cdot e^{-k^d_{Ph} \cdot t} \qquad (4a)$$

where $[Ph]_0$ is the initial phenol concentration, and k^d_{Ph} is the rate constant for phenol degradation. Equation 4a has been used for curve fitting. At $t \rightarrow 0$ the equation reduces to $[Ph] = [Ph]_0 \cdot (1 - k_{Ph}{}^d \cdot t)$, and the initial phenol degradation rate is $k^d_{Ph}[Ph]_0$.

The concentration of nitrophenols as a function of time is described by eq 4b

$$[NP] = \frac{k_{NP}{}^f \cdot [Ph]_0}{k_{NP}{}^d - k_{Ph}{}^d} \cdot (e^{-k^d_{Ph} \cdot t} - e^{-k^d_{NP} \cdot t}) \qquad (4b)$$

where NP stands for either 2-NP or 4-NP, and k^f_{NP} and k^d_{NP} are the rate constants for nitrophenol formation and degradation, respectively. The experimental data for nitrophenols have thus been fitted with eq 4b. At $t \rightarrow 0$ the equation reduces to $[NP]_{t\rightarrow 0} = k_{NP}{}^f \cdot [Ph]_0 \cdot t$, and the initial formation rate is $k^f_{NP}[Ph]_0$. The initial rates for phenol and nitrophenols are reported in Table 1, together with the associated standard errors.

Results and Discussion

Dissolved Fe(III). Fe(III) hydroxo complexes absorb near-UV radiation. Upon absorption, the complexes undergo photolysis with a generation of $^{\bullet}OH$ (*2*). The most photoactive species is $[Fe(OH)(H_2O)_5]^{2+}$ (*25*):

$$[Fe(OH)(H_2O)_5]^{2+} + h\nu + H_2O \rightarrow [Fe(H_2O)_6]^{2+} + {}^{\bullet}OH \quad [\Phi_{310\,nm} = 0.19] \qquad (5)$$

This species is the main ferric monomeric hydroxo complex in the pH interval 2.2−3.8, as calculated from reported stability constants (*26*). However, a mM solution of $Fe(ClO_4)_3$ at pH 3.0 is not stable, as the monomeric species slowly convert to polynuclear complexes and Fe(III) hydroxide colloids (*27*, *28*).

To distinguish the effects of monomeric, dimeric, or polymeric Fe(III) species as well as of iron hydroxide colloids, first we carried out irradiation at pH 1.5. Under such conditions, 95% of Fe(III) is present as $[Fe(H_2O)_6]^{3+}$ and the remaining 5% as $[Fe(OH)(H_2O)_5]^{2+}$. The prevailing species $[Fe(H_2O)_6]^{3+}$ can generate $^{\bullet}OH$ upon UV absorption (*25*):

$$[Fe(H_2O)_6]^{3+} + h\nu + H_2O \rightarrow [Fe(H_2O)_6]^{2+} + {}^{\bullet}OH + H^+ \quad [\Phi_{310\,nm} < 0.05] \qquad (6)$$

Taking into consideration the molar absorption coefficient ϵ of $[Fe(H_2O)_6]^{3+}$ ($\epsilon_{310\,nm} = 48\ M^{-1}\ cm^{-1}$) and $[Fe(OH)(H_2O)_5]^{2+}$

TABLE 1. Initial Degradation Rates for Phenol and Initial Formation Rates for 2- and 4-Nitrophenol[a]

no.	conditions	λ_{irr}, nm	pH	phenol degr. rate, M s^{-1}	2-NP form. rate, M s^{-1}	4-NP form. rate, M s^{-1}
1	$NaNO_2$ 0.0010 M	312	1.5	$(2.2 \pm 0.4) \times 10^{-8}$	$(8.7 \pm 1.0) \times 10^{-9}$	$(8.2 \pm 1.3) \times 10^{-9}$
2	$NaNO_2$ 0.0010 M + $Fe(ClO_4)_3$ 0.0066 M	312	1.5	$(1.1 \pm 0.1) \times 10^{-7}$	$(3.0 \pm 0.2) \times 10^{-8}$	$(2.0 \pm 0.1) \times 10^{-8}$
3	$Fe(ClO_4)_3$ 0.0066 M	312	1.5	$(1.5 \pm 0.1) \times 10^{-7}$	n/a[c]	n/a[c]
4	$Fe(ClO_4)_3$ 0.0066 M + 2-propanol 0.10 M	312	1.5	$(3.2 \pm 1.3) \times 10^{-9}$	n/a[c]	n/a[c]
5	$NaNO_2$ 0.0010 M	360	1.5	$(5.7 \pm 0.3) \times 10^{-8}$	$(1.4 \pm 0.1) \times 10^{-8}$	$(7.7 \pm 0.5) \times 10^{-9}$
6	$NaNO_2$ 0.0010 M + $Fe(ClO_4)_3$ 0.0066 M	360	1.5	$(1.2 \pm 0.1) \times 10^{-7}$	$(3.7 \pm 0.2) \times 10^{-8}$	$(1.7 \pm 0.2) \times 10^{-8}$
7	$Fe(ClO_4)_3$ 0.0066 M	360	1.5	$(1.8 \pm 0.3) \times 10^{-7}$	n/a[c]	n/a[c]
8	$Fe(ClO_4)_3$ 0.0066 M + 2-propanol 0.10 M	360	1.5	$(6.7 \pm 1.3) \times 10^{-9}$	n/a[c]	n/a[c]
9	$NaNO_2$ 0.0010 M + $Fe(ClO_4)_3$ 0.0066 M + 2-propanol 0.10 M	312	1.5	$(2.5 \pm 0.5) \times 10^{-8}$	$(1.0 \pm 0.1) \times 10^{-8}$	$(8.1 \pm 0.8) \times 10^{-9}$
10	$NaNO_2$ 0.0010 M + 2-propanol 0.10 M	312	1.5	$(3.4 \pm 0.4) \times 10^{-8}$	$(1.4 \pm 0.1) \times 10^{-8}$	$(9.1 \pm 0.4) \times 10^{-9}$
11	phenol 5.3×10^{-4} M + $Fe(ClO_4)_3$ 1.0×10^{-4} M	312	3.0	$(5.2 \pm 0.4) \times 10^{-9}$	n/a[c]	n/a[c]
12	phenol 5.3×10^{-4} M + $Fe(ClO_4)_3$ 1.0×10^{-4} M + 2-propanol 0.10 M	312	3.0	$(2.2 \pm 0.2) \times 10^{-9}$	n/a[c]	n/a[c]
13	phenol 5.3×10^{-4} M + $NaNO_2$ 0.001 M	312	3.0	$(1.6 \pm 0.3) \times 10^{-8}$	$(5.9 \pm 0.1) \times 10^{-9}$	$(4.0 \pm 0.1) \times 10^{-9}$
14	phenol 5.3×10^{-4} M + $NaNO_2$ 0.001 M + $Fe(ClO_4)_3$ 1.0×10^{-4} M	312	3.0	$(3.9 \pm 0.3) \times 10^{-8}$	$(7.4 \pm 0.9) \times 10^{-9}$	$(5.4 \pm 0.8) \times 10^{-9}$
15	phenol 5.3×10^{-4} M + $Fe(ClO_4)_3$ 1.0×10^{-4} M	312	4.0	$(3.8 \pm 0.3) \times 10^{-9}$	n/a[c]	n/a[c]
16	phenol 5.3×10^{-4} M + $Fe(ClO_4)_3$ 1.0×10^{-4} M + 2-propanol 0.10 M	312	4.0	$(1.8 \pm 0.1) \times 10^{-9}$	n/a[c]	n/a[c]
17	phenol 5.3×10^{-4} M + $NaNO_2$ 0.001 M	312	4.0	$(3.4 \pm 0.2) \times 10^{-9}$	$(7.6 \pm 0.5) \times 10^{-10}$	$(5.6 \pm 0.4) \times 10^{-10}$
18	phenol 5.3×10^{-4} M + $NaNO_2$ 0.001 M + $Fe(ClO_4)_3$ 1.0×10^{-4} M	312	4.0	$(5.8 \pm 0.1) \times 10^{-9}$	$(1.4 \pm 0.1) \times 10^{-9}$	$(9.8 \pm 0.5) \times 10^{-10}$
19	$NaNO_2$ 0.01 M	>430	6.0	$(1.1 \pm 0.2) \times 10^{-8}$	$(1.9 \pm 0.3) \times 10^{-9}$	$(1.4 \pm 0.2) \times 10^{-9}$
20	$NaNO_2$ 0.01 M + α-Fe_2O_3 0.20 g/L	>430	6.0	$(3.5 \pm 1.0) \times 10^{-8}$	$(1.8 \pm 0.2) \times 10^{-8}$	$(1.3 \pm 0.1) \times 10^{-8}$
21	$NaNO_2$ 0.01 M + β-FeOOH 0.20 g/L	>430	6.0	$(2.9 \pm 0.4) \times 10^{-8}$	$(1.4 \pm 0.1) \times 10^{-8}$	$(1.1 \pm 0.1) \times 10^{-8}$
22	α-Fe_2O_3 0.20 g/L	>430	6.0	$(3.5 \pm 2.9) \times 10^{-9}$	n/a[c]	n/a[c]
23	β-FeOOH 0.20 g/L	>430	6.0	$(1.1 \pm 0.8) \times 10^{-9}$	n/a[c]	n/a[c]
24	$NaNO_2$ 0.01 M, degas. N_2	>430	6.0	$(1.1 \pm 0.3) \times 10^{-8}$	$(1.2 \pm 0.2) \times 10^{-10}$	$(4.2 \pm 0.6) \times 10^{-11}$
25	$NaNO_2$ 0.01 M + α-Fe_2O_3 0.20 g/L, degas. N_2	>430	6.0	$(2.6 \pm 0.7) \times 10^{-9}$	$(6.5 \pm 0.4) \times 10^{-10}$	$(8.8 \pm 2.3) \times 10^{-10}$
26	$NaNO_2$ 0.01 M + β-FeOOH 0.20 g/L, degas. N_2	>430	6.0	$(6.0 \pm 1.5) \times 10^{-9}$	$(1.1 \pm 0.2) \times 10^{-9}$	$(1.3 \pm 0.3) \times 10^{-9}$
27	$NaNO_3$ 0.1 M	312	6.0	$(2.0 \pm 0.6) \times 10^{-8}$	$(1.2 \pm 0.1) \times 10^{-10}$	$(8.3 \pm 2.6) \times 10^{-11}$
28	$NaNO_2$ 0.004 M	312	6.0	$(8.6 \pm 2.3) \times 10^{-9}$	$(2.4 \pm 0.3) \times 10^{-10}$	$(4.1 \pm 0.1) \times 10^{-10}$
29	$NaNO_3$ 0.1 M + $NaNO_2$ 0.004 M	312	6.0	$(1.3 \pm 0.2) \times 10^{-8}$	$(4.0 \pm 0.1) \times 10^{-9}$	$(2.1 \pm 0.2) \times 10^{-9}$
30	humic acid 0.20 g/L	>430	6.0	$(6.3 \pm 0.5) \times 10^{-9}$	n/a[c]	n/a[c]
31	$NaNO_2$ 0.01 M + humic acid 0.20 g/L	>430	6.0	$(4.8 \pm 0.3) \times 10^{-9}$	*b*	*b*
32	$NaNO_3$ 0.1 M	>430	3.0	$(7.0 \pm 5.8) \times 10^{-10}$	*b*	*b*
33	$NaNO_3$ 0.1 M + humic acid 0.20 g/L	>430	3.0	$(5.0 \pm 0.6) \times 10^{-9}$	*b*	*b*
34	$NaNO_2$ 0.01 M	dark	3.0	$(7.7 \pm 0.3) \times 10^{-8}$	$(6.5 \pm 0.2) \times 10^{-9}$	$(3.0 \pm 0.3) \times 10^{-9}$
35	$NaNO_2$ 0.01 M + humic acid 0.20 g/L	dark	3.0	$(7.2 \pm 0.3) \times 10^{-8}$	$(6.9 \pm 0.2) \times 10^{-9}$	$(2.8 \pm 0.1) \times 10^{-9}$

[a] Conditions are reported in the table. Initial phenol concentration = 1.1×10^{-3} M, unless otherwise reported. [b] Nitrophenol formation was too low to be detected. [c] n/a: not applicable.

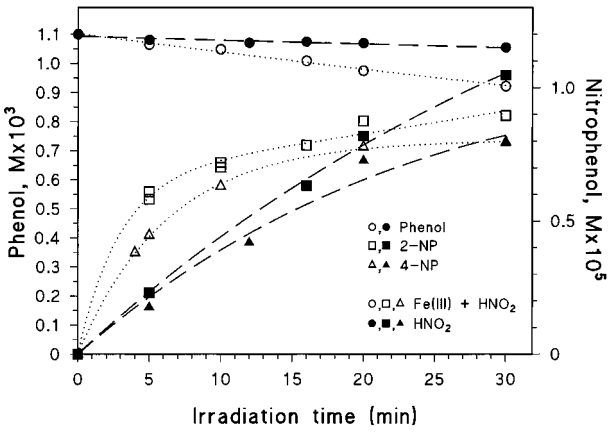

FIGURE 2. Phenol degradation and nitrophenol formation in the presence and in the absence of Fe(III). Initial conditions: 1.1×10^{-3} M phenol, 1.0×10^{-3} M $NaNO_2$, and 6.6×10^{-3} M $Fe(ClO_4)_3$ when present, pH 1.5, irradiation at 312 nm. Fitting curves drawn according to eq 4.

($\epsilon_{310\,nm} = 1826\ M^{-1}\,cm^{-1}$) (*25*), respectively, and the quantum yields for •OH photoformation at 310 nm (see reaction 5 and 6), the main source of •OH at pH 1.5 is $[Fe(OH)(H_2O)_5]^{2+}$.

Figure 2 shows the degradation of phenol and the formation of 2- and 4-nitrophenol (2-NP, 4-NP) upon 312 nm irradiation of phenol and $NaNO_2$, with and without the addition of $Fe(ClO_4)_3$ at pH 1.5, adjusted with the addition of $HClO_4$. In the presence of $Fe(ClO_4)_3$ the initial rate for nitrophenol formation is higher than in the presence of $NaNO_2$ alone, indicating that phenol nitration is enhanced by Fe(III) (see Table 1, entries #1 and #2).

In the presence of nitrite alone at pH 1.5, phenol nitration is due to a thermal processes involving HNO_2 (*15*), and possibly to the nitrous acid thermal dismutation, which yields •NO and $•NO_2$ (*29*). The photolysis of HNO_2 at 312 nm, also yielding $•NO_2$ (*6*), plays a minor role at pH 1.5 (*15*):

$$2HNO_2 \rightarrow •NO + •NO_2 + H_2O \quad [k_7 = 28.6\ M^{-1}\,s^{-1} \text{ at } 303\ K] \quad (7)$$

$$HNO_2 + h\nu \rightarrow •NO + •OH \quad [\Phi_{310} \approx 0.35] \quad (8)$$

$$•OH + HNO_2 \rightarrow •NO_2 + H_2O \quad [k_9 = 2.6 \times 10^9\ M^{-1}\,s^{-1}] \quad (9)$$

The thermal processes are likely to occur at the same extent both in the absence and in the presence of Fe(III), as they are independent from irradiation. The net effect of Fe(III) photolysis on the initial formation rates of both 2-NP and 4-NP can be evaluated as the difference between the rates in the presence of Fe(III) (Table 1, entry #2) and those in the absence of Fe(III) (Table 1, entry #1).

The enhanced nitrophenol formation rate in the presence of Fe(III) is most probably due to reactions 5 and 9, yielding $^{\bullet}NO_2$. Reaction 6, followed by reaction 9, may give a secondary contribution. Reaction 9 between $^{\bullet}OH$ and HNO_2 is in competition with the reaction between $^{\bullet}OH$ and phenol (rate constant 1.4×10^{10} M^{-1} s^{-1} (*30*)). At phenol and HNO_2 concentrations of 1.1×10^{-3} M and $\approx 1.0 \times 10^{-3}$ M, respectively, 86% of photoformed $^{\bullet}OH$ should react with phenol and 14% with HNO_2, based on above given kinetic constants. For this reason the initial degradation rate of phenol is higher in the presence of Fe(III) + HNO_2 than in the presence of HNO_2 alone (Table 1, entries #1 and #2). For the same reason, degradation of nitrophenols is faster in the presence of Fe(III) + HNO_2 than in the case of HNO_2 alone. The time evolution of both 2-NP and 4-NP for the first 30 min irradiation is almost linear in the case of HNO_2 alone, indicating that the degradation rate is lower than the formation rate (see Figure 2). On the contrary, the concentration vs time curves of both 2-NP and 4-NP reach a plateau after about 10 min of irradiation in the presence of Fe(III). The plateau indicates that the degradation rate equals the formation rate, thus formation and transformation of nitrophenols are both enhanced by Fe(III).

The role of $^{\bullet}OH$, according to reactions 5 and 9, is further supported by the degradation of phenol upon 312 nm irradiation in the presence of 2-propanol. This alcohol is an $^{\bullet}OH$ scavenger (*31*), with a rate constant 3.0×10^9 M^{-1} s^{-1} with $^{\bullet}OH$ radical (*30*). In the presence of 1.1×10^{-3} M phenol and 0.10 M 2-propanol, 95% of photoformed $^{\bullet}OH$ would react with 2-propanol and 5% with phenol. This calculation is in agreement with the ratio experimentally evaluated (see entries #3 and #4 in Table 1). It can be concluded that a relevant $^{\bullet}OH$ photoproduction takes place in the system and that the nitration occurs via reaction 9.

The addition of $NaNO_2$ to an $Fe(ClO_4)_3$ solution induces a small change in the solution absorption spectrum, which cannot be explained by the mere overlapping between the $NaNO_2$ and $Fe(ClO_4)_3$ spectra. This change is most likely due to the formation of the complex $FeNO_2^{2+}$. Photolysis of $FeNO_2^{2+}$ might contribute to $^{\bullet}NO_2$ photoformation according to

$$FeNO_2^{2+} + h\nu \rightarrow Fe^{2+} + {}^{\bullet}NO_2 \qquad (10)$$

Reaction 10 may be postulated in analogy to the photolysis of $FeSO_4^+$ yielding $^{\bullet}SO_4^-$ (*25*):

$$FeSO_4^+ + h\nu \rightarrow Fe^{2+} + {}^{\bullet}SO_4^- \quad [\Phi_{310\ nm} = 0.0035] \qquad (11)$$

Although the quantum yield of reaction 11 is very low, the quantum yield for reaction 10 could be higher comparing the monoelectronic reduction potentials of $^{\bullet}NO_2/NO_2^-$ and $^{\bullet}SO_4^-/SO_4^{2-}$, which are 1.0 and 2.4 V, respectively (*32*). As $FeNO_2^{2+}$ the complex $FeSO_4^+$ absorbs in the UV region ($\epsilon_{310\ nm} = 1826\ M^{-1}\,cm^{-1}$) (*25*). Calculations using reported stability constants (*26*) show that in a solution containing 0.0066 M $Fe(ClO_4)_3$ and 0.0010 M $NaNO_2$, at pH 1.5 for $HClO_4$, $[Fe^{3+}] \approx 6.2 \times 10^{-3}$ M, $[FeOH^{2+}] \approx 4.2 \times 10^{-4}$ M, and $[FeNO_2^{2+}] \approx 1.7 \times 10^{-5}$ M. Since $[FeNO_2^{2+}]$ is negligible with respect to the concentration of other Fe(III) species, the $FeNO_2^{2+}$ spectrum was obtained by spectra subtraction. It shows a broad maximum around 298 nm, with a tail until 400 nm. Using calculated concentrations, the molar extinction coefficient at 312 nm is 6.1×10^3 M^{-1} cm^{-1}. The absorptances at 312 nm as calculated from eq 3b are $\alpha_{Fe(III)} = 0.60$, $\alpha_{HNO2} = 0.0027$, and $\alpha_{Fe(NO2)2+} = 0.058$.

For discriminating the effect of reaction 10, one may use the different absorption of $FeNO_2^{2+}$ observed at 360 nm ($\epsilon_{360\ nm} \approx 0.2 \times \epsilon_{312\ nm}$). Taking into account the photon flux of the two lamps, the rate of photon absorption by the complex is very similar at 312 nm (9.2×10^{-9} Ein s^{-1}) and 360 nm (8.8×10^{-9} Ein s^{-1}). As the observed rates of nitrophenol formation at 360 nm are comparable to those observed at 312 nm (see entries #2 and #6), reaction 10 can account for the effect of Fe(III) photoexcitation only if the quantum yield is almost equal at both the wavelengths and ≥ 0.22. This is unlikely because at higher wavelengths the quantum yield is normally lower, as it is the case for example of reaction 11 ($\Phi_{350\ nm} = 0.0015$) (*25*). As a consequence, the reactions 5, 6, and 9 account for nitrophenol formation better than reaction 10. In addition, phenol degradation experiments performed with Fe(III) alone and with Fe(III) + 2-propanol indicate that the rates of $^{\bullet}OH$ photoproduction are similar for irradiation at 312 nm (entries #3 and #4) and at 360 nm (entries #7 and #8). As a consequence, the results are better explained by reactions 5, 6, and 9 rather than by reaction 10.

A second experiment, in which 2-propanol was added to the phenol/HNO_2/ Fe(III) system under irradiation at 312 nm, was also carried out. As the alcohol is an $^{\bullet}OH$ scavenger, it should inhibit reaction 9 without a relevant influence on reaction 10. The addition of 2-propanol in the presence of Fe(III) and HNO_2 reduces the initial formation rates of 2-NP and 4-NP (see Table 1, entry #9, and compare with entry #2), which become very similar to those observed in the presence of HNO_2 alone (compare entries #9 and #1). The comparison of entries #10 and #1 indicates that 2-propanol does not inhibit the thermal nitration of phenol. Thus, in the presence of Fe(III) + HNO_2 + 2-propanol the reaction proceeds only via the thermal decomposition of HNO_2. As a consequence, the enhancement of nitrophenol formation by Fe(III) is linked to the photoproduction of $^{\bullet}OH$, and reaction 10 plays a negligible role in the system.

The significance of the reaction pathway involving the oxidation of the nitrosoderivatives was also assessed. The reactive species for phenol nitrosation is N_2O_3, which transforms phenol into 4-NOP (*33*). Upon nitrite photolysis, a fraction of 4-NOP is transformed into 4-NP (*14*). Control experiments showed that dissolved Fe(III) under irradiation in the presence of nitrite does not transform 4-NOP into 4-NP to a higher extent than NO_2^- alone. Furthermore, in both cases, the production of 4-NP was very limited. This suggests that the enhanced nitrophenol formation in the presence of Fe(III) + nitrite with respect to nitrite alone does not involve the nitrosoderivative pathway.

A second set of experiments was carried out at pH 3.0 (pH adjusted by the addition of $HClO_4$). Although for experimental convenience the concentration of $Fe(ClO_4)_3$ was reduced, and $[Fe(OH)(H_2O)_5]^{2+}$ would be the main Fe(III) species in the system, the presence of possible dimeric and polymeric iron species could not be excluded. In addition to reactions 5 and 6, which are characteristic of mononuclear Fe(III) species, the following excitation and electron-transfer processes for di- and polymeric species may be postulated for phenol under these conditions, as suggested for 2,6-dimethylphenol (*28*):

$$[Fe^{III}] + h\nu \rightarrow [Fe^{III}]^* \qquad (12)$$

$$[Fe^{III}]^* + PhOH \rightarrow Fe^{2+} + PhO^{\bullet} + H^+ \qquad (13)$$

Although $^{\bullet}OH$ radicals are efficiently scavenged by 2-propanol, no reaction has been detected between 2-propanol and $[Fe^{III}]^*$ (*28*). Thus, the effect of 2-propanol on the initial phenol degradation rate at pH 3.0 still gives indication on the production of $^{\bullet}OH$. Table 1 reports the initial phenol degradation rate in the absence (entry #11) and in the presence (entry #12) of 0.10 M 2-propanol. The alcohol lowers the rate of about 2.4 times. This indicates that a moderate $^{\bullet}OH$ photoproduction takes place in the system along with direct electron transfer to $[Fe^{III}]^*$ (reaction 13). This process should have a role also in the production of $^{\bullet}NO_2$ via reaction

14, since $E°$ ($^{\bullet}NO_2/NO_2^-$) = 1.0 V (*32*) and $E°$ ($PhOH^{\bullet+}$/PhOH) = 0.97 (*34*).

$$[Fe^{III}]^* + NO_2^- \rightarrow Fe^{2+} + {}^{\bullet}NO_2 \qquad (14)$$

In addition to reaction 14, a further contribution to phenol nitration may come from the phenoxyl radical via reaction 15 (*8*, *10*).

$$PhO^{\bullet} + {}^{\bullet}NO_2 \rightarrow O_2N{-}Ph\text{-}OH \qquad (15)$$

Experiments have been carried out also in the presence of 1.0×10^{-3} M nitrite. Table 1 reports the initial rates of phenol degradation and nitrophenol formation for nitrite alone (entry #13) and for Fe(III) + nitrite (entry #14). At pH 3.0, 60% of nitrite is present as HNO_2 and 40% as NO_2^- as calculated using reported stability constants (*26*). The absorption spectra of Fe(III), HNO_2, and NO_2^- are reported in Figure 1. Samples were irradiated at 312 nm. Light absorption calculations, performed according to eq 3b, showed that in a solution containing 1.0×10^{-4} M Fe(III) and 1.0×10^{-3} M nitrite at pH 3.0, the absorptances are α_{Fe} = 0.057 and α_{NO2} = 0.005 for Fe(III) and nitrite + HNO_2, respectively. This means that also at pH 3.0 the reaction 5 prevails over reactions 1 and 8.

The initial rate of nitrophenol formation is slightly higher in the Fe(III) + nitrite case, consistently with the role played by reactions 5, 2, and 9, but the difference is limited. The non-negligible rate of nitrophenol formation in the presence of nitrite alone at pH 3.0, contributing for almost 80% of the NP formation rate observed in the presence of Fe(III) species, may be ascribed to the thermal process depicted in reaction 7.

To limit the role of reaction 7, a third set of experiments was carried out at pH 4.0. Under such conditions, [NO_2^-] (88% of total nitrite) prevails over [HNO_2] (12%), $[Fe(OH)_2(H_2O)_4]^+$ (61% of the total mononuclear Fe(III)) prevails over $[Fe(OH)(H_2O)_5]^{2+}$ (38%) and $[Fe(H_2O)_6]^{3+}$(1%), and the absorption spectrum of Fe(III) slightly changes (see Figure 1). Absorbed light calculations give α_{Fe} = 0.047 and α_{NO2} = 0.008, comparable to those previously calculated at pH 3.0. To assess the extent of $^{\bullet}OH$ generation (reaction 5), phenol was irradiated in the presence of Fe(III) at pH 4.0, with and without 2-propanol 0.10 M. Table 1 reports the initial phenol degradation rate in the absence (entry #15) and in the presence (entry #16) of 0.10 M 2-propanol. The alcohol lowers the rate of about 2.1 times. The comparison of the effect of 2-propanol on the initial phenol degradation rate at pH 1.5, 3.0, and 4.0 indicates that the role of reactions 5 and 6 decreases as pH increases.

The degradation of phenol and the formation of 2- and 4-nitrophenol upon 312 nm illumination at pH 4.0, with and without addition of 1.0×10^{-4} M $Fe(ClO_4)_3$, are reported in Figure 3. Initial rates are listed in Table 1 (entries #17 and #18). The initial rates of nitrophenol formation are almost double in the presence of iron species. The formation of nitrophenols accounts in both cases for about 40% of the initial phenol transformation. Conclusions

In summary, illumination of aqueous Fe(III) solutions produces $^{\bullet}OH$, which can then oxidize NO_2^- and HNO_2 to nitrogen dioxide (reaction 5, 6, 2, and 9). The Fe(III)-photoinduced production of $^{\bullet}NO_2$ largely dominates photolysis of both nitrite and nitrous acid (reactions 1, 2, 8, and 9) as well as the thermal dismutation of nitrous acid (reaction 7). However, measurements carried out in the presence of an $^{\bullet}OH$ scavenger show that the production of $^{\bullet}OH$ upon Fe(III) illumination (reactions 5 and 6) decreases as pH increases. The fraction of photoinduced processes not accounted for by $^{\bullet}OH$ production is attributed to direct electron transfer to $[Fe^{III}]^*$ (reactions 12 and 13 and possibly

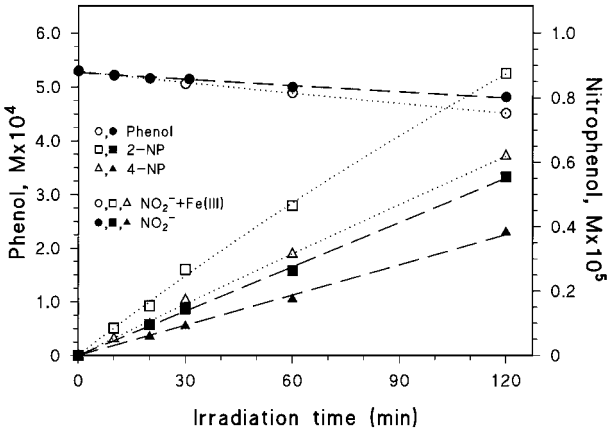

FIGURE 3. Phenol degradation and nitrophenol formation in the presence and in the absence of Fe(III). Initial conditions: 5.3×10^{-4} M phenol, 1.0×10^{-3} M $NaNO_2$, and 1.0×10^{-4} M $Fe(ClO_4)_3$ when present, pH 4.0, irradiation at 312 nm. Fitting curves drawn according to eq 4.

14 and 15). The role of these reactions increases as pH increases. At environmental acidic pH values, these reactions play a significant role.

α-Fe_2O_3 and β-FeOOH. These oxides are semiconductors with indirect band gap absorption in the visible region. Hematite absorbs radiation at λ < 530 nm (band gap 2.3 eV (*35*)). The band gap for β-FeOOH was reported to be 2.12 eV (*21*), corresponding to an absorption at λ < 575 nm. The photocatalytic behavior of α-Fe_2O_3 (hematite) has been widely studied and the mechanism of some of its photoreactions elucidated (*21*, *35*−*38*). Upon absorption, electrons are promoted from the valence (VB) to the conduction band (CB), leaving holes in the valence band:

$$\alpha\text{-}Fe_2O_3 + h\nu \rightarrow e^-_{CB} + h^+_{VB} \qquad (16)$$

Electrons and holes can quickly recombine or react with dissolved molecules. Radiative excitation can also result in charge-transfer reactions, involving surficial species (*37*):

$$\equiv Fe^{III}\text{-}OH + h\nu \rightarrow Fe^{2+}_{aq} + {}^{\bullet}OH \qquad (17)$$

Reaction 17 can induce oxidation of natural or xenobiotic compounds via photoformed $^{\bullet}OH$ and causes photocorrosion of α-Fe_2O_3.

Since nitrite absorbance has a maximum at 354 nm and becomes negligible above 420 nm, to excite iron oxides almost selectively, the suspensions were illuminated with a Xenon lamp equipped with a 430 nm filter. Under these conditions reaction 17 is expected to play a minor role, as it takes place upon excitation of a charge-transfer band with band gap = 3.3 eV (λ = 375 nm (*37*)).

Figure 4 shows the degradation of phenol and the formation of 2- and 4-NP when 1.1×10^{-3} M phenol is illuminated in the presence of 0.01 M $NaNO_2$ (pH 6), in homogeneous phase and in the presence of the colloidal ferric oxides (0.20 g/L). The initial rates of nitrophenol formation are significantly higher in the presence of the oxides than in homogeneous phase (see entries #19−21). The formation of nitrophenols in homogeneous phase is due to the residual nitrite absorption (see Figure 1). Moreover, the formation of nitrophenols accounts for 30% of initial phenol transformation in the case of nitrite alone, 90% in the presence of α-Fe_2O_3, and 85% in the presence of β-FeOOH (see Table 1, entries #19−21). Thus, photoexcitation of colloidal iron oxides in the presence of nitrite and at environmentally significant conditions leads to a sustained production of

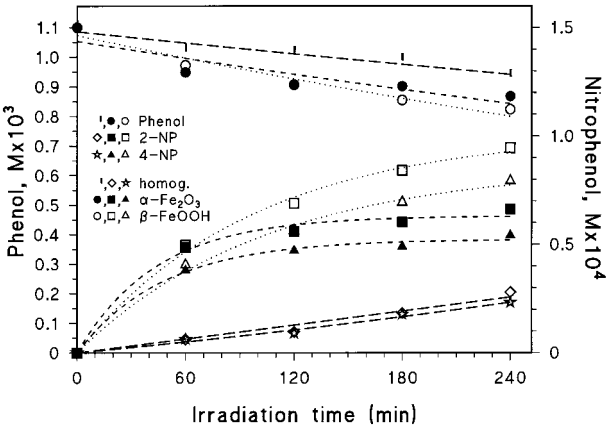

FIGURE 4. Phenol degradation and nitrophenol formation in the presence and in the absence of iron oxides. Initial conditions: 1.1 × 10^{-3} M phenol, 0.01 M $NaNO_2$ (pH 6), irradiation under Solarbox + 430-nm filter. Fitting curves drawn according to eq 4.

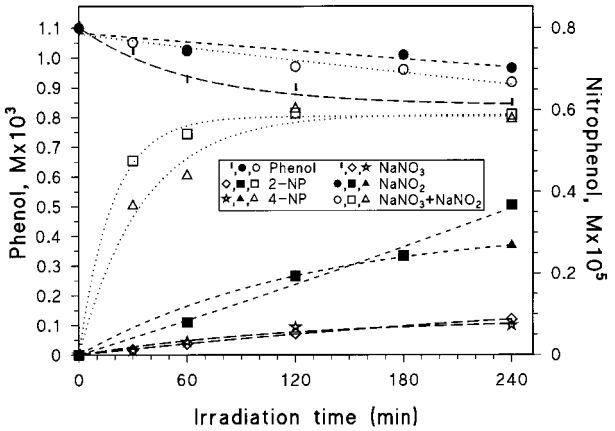

FIGURE 5. Phenol degradation and nitrophenol formation in the presence and in the absence of nitrate and nitrite. Initial conditions: 1.1 × 10^{-3} M phenol, 0.1 M $NaNO_3$, and 4.0 × 10^{-3} M $NaNO_2$ (pH 6), irradiation at 312 nm. Fitting curves drawn according to eq 4.

nitrophenols. In the presence of the iron oxides alone, without nitrite, very low photoinduced transformation of phenol was observed, as the measured initial degradation rates show (Table 1, entries #22 and #23).

As already done in the case of dissolved Fe(III), the role of the pathway of nitrophenol formation upon oxidation of the nitrosoderivatives (*14*) had to be assessed. 4-NOP was not detected under the present experimental conditions, neither in the presence of $NaNO_2$ alone nor in the slurries iron oxide + nitrite. This could be due to a slow formation rate or to a fast degradation rate. Control experiments on 2 × 10^{-5} M 4-NOP in these systems showed that the degradation rate of 4-NOP is not significantly different from that observed in the presence of 0.1 M $NaNO_2$ (pH 6.5, irradiation at 360 nm (*14*)). The irradiation of 1.1 × 10^{-3} M phenol + 0.1 M $NaNO_2$ at 360 nm gave relevant amounts of 4-NOP, differently from the systems containing $NaNO_2$ alone or with iron oxides, irradiated at > 430 nm. The lack of detection of this compound in the presence of $NaNO_2$ alone or iron oxides suggests that the 4-NOP formation rate is low. Thus, a conceivable nitrosoderivative pathway cannot explain the effect of iron oxides.

The main reaction mechanism in semiconductor slurries should involve oxidation of surface adsorbed nitrite by photoformed holes:

$$h^+_{VB} + NO_2^- \rightarrow {}^\bullet NO_2 \qquad (18)$$

This process is thermodynamically allowed because at pH 7 E ($^\bullet NO_2/NO_2^-$) = 1.0 V (*32*). Faust et al. (*35*) reported E_{VB} = 2.3 V for α-Fe_2O_3. The data by Leland and Bard (*21*) allow for roughly evaluating E_{VB} = 2.6−2.9 V for β-FeOOH.

For reaction 18 to take place, a parallel process of scavenging of e^-_{CB} has to occur. No reduction of Fe(III) was detected as Fe(II)/1,10-phenathroline complex in aqueous solution under illumination > 430 nm. A considerable (>90%) inhibition in nitrophenol formation is detected when oxygen is purged with a stream of high purity nitrogen from the oxide slurry before irradiation. Moreover, the initial degradation rates for phenol in the absence of oxygen are lower than in aerated solution in the case of the slurries (see Table 1, entries #25 and #26 compared with entries #20 and #21), while practically no difference was observed in the presence of nitrite alone. Thus, oxygen should have a role in the photocatalytic system. Direct electron scavenging by free dissolved oxygen is not allowed (at pH 7, E_{CB} = 0.0 V for α-Fe_2O_3 (*35*) and 0.5−0.7 V for β-FeOOH (*21*), while E ($O_2/{}^\bullet O_2^-$) = − 0.33 V (*32*)). However, conduction band electrons could still reduce surface-bound dioxygen, as is the case for the photocatalytic oxidation of sulfur dioxide to sulfate in α-Fe_2O_3 slurries (*35*). Surface-bound oxygen was shown to react with surficial sulfur-containing radicals, acting as an indirect electron scavenger. As in our case, the photocatalytic process was favored in the presence of oxygen.

In conclusion, iron oxides and nitrite show mutual interaction, as indicated by the enhancement of both the nitrophenol formation and the overall phenol transformation rates, if compared with systems in which they are present separately. Most likely, the interaction is due to the oxidation of nitrite to nitrogen dioxide by electron vacancies on the irradiated oxides.

Nitrate. The ion NO_3^- absorbs near UV radiation (absorption maximum at 302 nm). Absorption causes photolysis according to reaction 19, followed by reaction 1b (*31*):

$$NO_3^- + h\nu \rightarrow {}^\bullet NO_2 + {}^\bullet O^- \quad [\Phi_{310\ nm} \approx 0.01] \qquad (19)$$

In the presence of nitrite, the radical $^\bullet$OH formed upon nitrate photolysis can be involved in reaction 2, oxidizing nitrite to nitrogen dioxide. This should add to the $^\bullet NO_2$ produced by nitrate photolysis, enhancing phenol nitration.

To gain information about the role of nitrate photolysis, nitrite should not be excited. The illumination of 0.1 M nitrate in the presence of 0.004 M nitrite at 312 nm partially fulfills this requirement (see Figure 1). Calculations performed according to eq 3b under the used experimental conditions indicate that the absorptance of 0.1 M nitrate is α_{NO3} = 0.450 when it is alone, and α_{NO3} = 0.443 in the presence of 0.004 M nitrite. The absorptance of 0.004 M nitrite is inhibited in the presence of nitrate (α_{NO2} = 0.036 when nitrite is alone and α_{NO2} = 0.027 in the presence of 0.1 M nitrate).

Figure 5 reports the degradation of phenol and the formation of 2-NP and 4-NP in the presence of 0.004 M nitrite alone, 0.1 M nitrate alone, and the mixture nitrate + nitrite. The results indicate that under almost selective photoexcitation of nitrate nitrophenols form in much larger amounts in the presence of the mixture $NaNO_3$ + $NaNO_2$ than in the other cases (see Table 1, entries #27−29). Formation of nitrophenols accounts for 1% of initial phenol transformation in the presence of nitrate alone, 8% in the presence of nitrite alone, and 45% in the mixture. It can be inferred that nitrite enhances the formation of nitrophenols under conditions of nitrate photolysis. The results are consistent with the hypothesis that the photolysis of nitrate in the presence of nitrite leads to the generation of $^\bullet NO_2$ according to reactions 19, 1b, and 2. The scavenging of $^\bullet$OH by nitrite (reaction 2) makes clear why the initial phenol degradation rate in the

presence of nitrate + nitrite (1.3×10^{-8} M s^{-1}) is lower than in the case of nitrate alone (2.0×10^{-8} M s^{-1}).

Since a faster conversion of 4-NOP into 4-NP was observed in the presence of nitrate + nitrite (55% conversion after 2 h irradiation) than in the presence of nitrite alone (20% conversion after the same irradiation time), the pathway involving the oxidation of the nitrosoderivatives may have a more important role in the process of phenol nitration in the presence of nitrate + nitrite than in the presence of nitrite alone. However, no 4-NOP was detected when phenol was irradiated in the presence of 0.004 M $NaNO_2$ and of 0.004 M $NaNO_2$ + 0.1 M $NaNO_3$. The transformation rate of 4-NOP observed in these systems is not significantly different from that observed in systems in which relevant formation of 4-NOP occurs (*14*). Thus, the lack of detection of 4-NOP in the presence of $NaNO_2$ and of the mixture $NaNO_2$ + $NaNO_3$ is due to a slow formation rate rather than to a fast transformation rate. As a consequence, the fairly high yield of oxidation of 4-NOP to 4-NP in the presence of nitrate + nitrite cannot give a significant contribution to the overall formation of 4-NP, due to the negligible formation of 4-NOP.

These findings suggest that, under conditions of nitrate photoexcitation, the nitration of phenol in the mixture nitrate + nitrite is enhanced by the oxidation of nitrite to nitrogen dioxide due to •OH radicals generated by nitrate photolysis.

Humic Acids. Humic substances constitute a relevant fraction (30−60%) of dissolved organic matter. They are a biologically refractory, reddish-brown material and originate from the decomposition of vegetal organic matter (*39*). Their ubiquitous diffusion in natural waters, together with their ability to absorb a consistent fraction of sunlight, makes them a potentially important environmental factor when photoinduced processes are considered (*2*, *40*, *41*). Humic acids (HS) are involved in the iron redox cycling in surface waters (*42*). The absorption of radiation by HS promotes the transition to the first excited singlet state, which partially converts to the reactive excited triplet state. The latter can induce production of solvated electrons and singlet oxygen and conversion of the ground singlet states of some organic substances into excited triplets (*2*). Humic acids thus play the role of photosensitizers for many reactions of environmental importance.

Nitrite, humic acids, and their mixture have been illuminated under the Xenon lamp, equipped with 430 nm filter (see entries #30 and #31). The illumination of a mixture of nitrite and humic acids in the presence of phenol does not produce nitrophenols. On the contrary, the photolysis of nitrite alone under the lamp yields some nitrophenols (see entry #19). These results indicate that humic acids inhibit nitrite photolysis, thus impeding nitrogen dioxide and nitrophenol formation under the adopted experimental conditions.

Humic acids and nitrate were also illuminated under the same light source (pH 3.0 with HNO_3, see entries #32 and #33). Aquated electrons formed under photoexcitation of HS could react with nitrate according to (*43*):

$$NO_3^- + e^-_{aq} \rightarrow {}^{\bullet}NO_3^{2-} \quad [k_{20} = 9.7 \times 10^9\ M^{-1}\ s^{-1}] \quad (20)$$

$${}^{\bullet}NO_3^{2-} + H_2O \rightarrow {}^{\bullet}NO_2 + 2OH^- \quad [k_{21} = 1 \times 10^3\ s^{-1}] \quad (21)$$

The formation of $^{\bullet}NO_2$ via reactions 20 and 21 should enhance phenol nitration. However, no detectable formation of nitrophenols was detected upon irradiation of nitrate and humic acids at $\lambda > 430$ nm, indicating either a low yield for the formation of e^-_{aq}, or additional depletion processes that dominate reaction 20.

The interpretation of the results obtained with both nitrite and nitrate should be different if humic acids were a sink of $^{\bullet}NO_2$. This has been controlled in the case of phenol nitration due to the thermal decomposition of HNO_2. Since this process occurs in the dark, competition for light absorption by humic acid is not an issue. A negligible effect on the rate of nitrophenol formation in the dark due to the presence of humic acids was observed in the presence of $NaNO_2$ 0.01 M, at pH 3.0 (see Table 1, entries #34 and #35). This result allows for the exclusion of the hypothesis that humic acids react with nitrogen dioxide.

Environmental Significance. The interactions between different environmental factors are of paramount importance in the understanding of environmental processes. Photoreactions of environmentally ubiquitous dissolved iron(III), iron oxides, and nitrate lead to the oxidation of NO_2^-/HNO_2 to $^{\bullet}NO_2$ and give a new pathway for the $^{\bullet}NO_2$-promoted nitration of organic matter, either natural or xenobiotic. These processes are quite different from those involving direct photolysis of nitrite, which mainly generates •OH leading to oxidation of organic molecules (*2*, *5*, *7*), and add new relevant pathways to the complex chemistry of environmental compartments, such as natural aquifers and atmospheric aerosols, in the presence of sunlight.

Acknowledgments

Financial support of CNR, MURST, Inter-University Consortium "Chemistry for the Environment" (INCA), PNRA Progetto Antartide and Università di Torino—Progetto Giovani Ricercatori is kindly appreciated.

Literature Cited

(1) Hoigné, J. In *Aquatic Chemical Kinetics*; Stumm, W., Ed.; John Wiley & Sons: New York, 1990; pp 43−70.
(2) Boule, P.; Bolte, M.; Richard, C. In *The Handbook of Environmental Chemistry Vol. 2.L* (*Environmental Photochemistry*); Boule, P., Ed.; Springer-Verlag: Berlin, 1999; pp 181−215.
(3) Beitz, T.; Bechmann, W.; Mitzer, R. *Chemosphere* **1999**, *38*, 351−361.
(4) Vaughan, P. P.; Blough, N. V. *Environ. Sci. Technol.* **1998**, *32*, 2947−2953.
(5) Arakaki, T.; Miyake, T.; Hirakawa, T.; Sakugawa, H. *Environ. Sci. Technol.* **1999**, *33*, 2561−2565.
(6) Fischer, M.; Warneck, P. *J. Phys. Chem.* **1996**, *100*, 18749−18756.
(7) Machado, F.; Boule, P. *J. Photochem. Photobiol. A: Chem.* **1995**, *6*, 73−80.
(8) Coombes, R. G.; Diggle, A. W.; Kempsell, S. P. *Tetrahedron Lett.* **1994**, *35*, 6373−6376.
(9) Dzengel, J.; Theurich, J.; Bahnemann, D. *Environ. Sci. Technol.* **1999**, *33*, 294−300.
(10) Vione, D.; Maurino, V.; Minero, C.; Vincenti, M.; Pelizzetti, E. *Chemosphere* **2001**, *44*, 237−248.
(11) Guillaume, D.; Morvan, J.; Martin, G. *Environ. Technol. Lett.* **1989**, *10*, 491−500.
(12) Eberhardt, M. K. *J. Phys. Chem.* **1975**, *79*, 1067−1069.
(13) Pitts, J. N.; Arey, J. S.; Zielinska, B.; Winer, A. M.; Atkinson, R. *Atmos. Environ.* **1985**, *19*, 1601−1608.
(14) Vione, D.; Maurino, V.; Minero, C.; Pelizzetti, E. *Chemosphere* **2001**, *45*, 893−902.
(15) Vione, D.; Maurino, V.; Minero, C.; Pelizzetti, E. *Chemosphere* **2001**, *45*, 903−910.
(16) *Photocatalysis. Fundamentals and Applications*; Serpone, N., Pelizzetti, E., Eds.; John Wiley & Sons: New York, 1989.
(17) Minero, C.; Mariella, G.; Maurino, V.; Pelizzetti, E. *Langmuir* **2000**, *16*, 2632−2641.
(18) Arey, J. In *PAHs and related compounds*; Neilson, A. H., Ed.; Springer: Berlin, 1998; pp 347−380.
(19) Leuenberger, C.; Czuczwa, J.; Tremp, J.; Giger, W. *Chemosphere* **1988**, *17*, 511−515.
(20) Enya, T.; Suzuki, H.; Watanabe, T.; Hirayama, T.; Himasatsu, Y. *Environ. Sci. Technol.* **1997**, *31*, 2772−2776.
(21) Leland, J. K.; Bard, A. J. *J. Phys. Chem.* **1987**, *91*, 5076−5083.
(22) Calvert, J. G.; Pitts, J. N. *Photochemistry*; John Wiley & Sons: New York, 1966; pp 780−786.
(23) Glossary of Terms Used in Photochemistry. *Pure Appl. Chem.* **1996**, *12*, 2223−2286.
(24) Leifer, A. *The Kinetics of Environmental Aquatic Photochemistry*; ACS: 1988.
(25) Benkelberg, H.-J.; Warneck, P. *J. Phys. Chem.* **1995**, *99*, 5214−5221.

(26) Smith, R. M.; Martell, A. E.; Motekaitis R. J. NIST *Critical Selected Stability Constant of Metal Complexes Database, Ver. 5.0*; 1998.
(27) Faust, B. C.; Hoigné, J. *Atmos. Environ.* **1990**, *24A*, 79−89.
(28) Mazellier, P.; Mailhot, G.; Bolte, M. *New J. Chem*. **1997**, *21*, 389−397.
(29) Park, J.-Y.; Lee, Y.-N. *J. Phys. Chem*. **1988**, *92*, 6294−6302.
(30) Buxton, G. V.; Greenstock, C. L.; Helman, W. P.; Ross, A. B. *J. Phys. Chem. Ref. Data* **1988**, *17*, 1027−1284.
(31) Warneck, P.; Wurzinger, C. *J. Phys. Chem*. **1988**, *92*, 6278−6283.
(32) Wardman, P. *J. Phys. Chem. Ref. Data* **1989**, *18*, 1637−1755.
(33) Pires, M.; Rossi, M. J.; Ross, D. S. *Int. J. Chem. Kinet.* **1994**, *26*, 1207−1227.
(34) Alfassi, Z. B.; Hue, R. E.; Neta, P.; Shoute, C. T. *J. Phys. Chem*. **1990**, *94*, 8800−8805.
(35) Faust, B. C.; Hoffmann, M. R.; Bahnemann, D. W. *J. Phys. Chem*. **1989**, *93*, 6371−6381.
(36) Siffert, C.; Sulzberger, B. *Langmuir* **1991**, *7*, 1627−1634.
(37) Faust, B. C.; Hoffmann, M. R. *Environ. Sci. Technol.* **1986**, *20*, 943−948.
(38) Waite, T. D.; Morel, F. M. M. *Environ. Sci. Technol.* **1984**, *18*, 860−868.
(39) Thurman, E. M. *Organic Geochemistry of Natural Waters*; Martinus Nijhoff/DR Junk: Boston, 1985.
(40) Canonica, S.; Jans, U.; Stemmler, K.; Hoigné, J. *Environ. Sci. Technol.* **1995**, *29*, 1822−1831.
(41) Canonica, S.; Hoigné, J. *Chemosphere* **1995**, *30*, 2365−2374.
(42) Voelker, B. M.; Morel, F. M. M.; Sulzberger, B. *Environ. Sci. Technol.* **1997**, *31*, 1004−1011.
(43) Løgager, T.; Sehested, K. *J. Phys. Chem*. **1993**, *97*, 10047−10052.

Received for review April 9, 2001. Revised manuscript received October 4, 2001. Accepted October 4, 2001.

ES010101C